Tailoring the electrical conductivity of GaAs by nitrogen incorporation

2009 J. Phys.: Condens. Matter 21 174209

(http://iopscience.iop.org/0953-8984/21/17/174209)

J. Phys.: Condens. Matter **21** (2009) 174209 (7pp) doi:10.1088/0953-8984/21/17/174209

Tailoring the electrical conductivity of GaAs by nitrogen incorporation

A Patanè[1], G Allison[1], L Eaves[1], M Hopkinson[2], G Hill[2] and A Ignatov[3]

[1] School of Physics and Astronomy, University of Nottingham, Nottingham NG7 2RD, UK
[2] Department of Electronic and Electrical Engineering, University of Sheffield, Sheffield S3 3JD, UK
[3] Institute for Physics of Microstructures, Russian Academy of Sciences, 603950 Nizhny Novgorod, Russia

E-mail: amalia.patane@nottingham.ac.uk

Received 1 October 2008, in final form 23 October 2008
Published 1 April 2009
Online at stacks.iop.org/JPhysCM/21/174209

Abstract

We investigate the electrical conductivity of the dilute nitride alloy $GaAs_{1-x}N_x$, focusing on the range of concentrations of N over which this material system behaves as a good conductor. We report a large increase of the resistivity for $x > 0.2\%$ and a strong reduction of the electron mobility, μ, at $x \sim 0.1\%$. In the ultra-dilute regime ($x \sim 0.1\%$) and at low electric fields (<1 kV cm^{-1}), the electrical conductivity retains the characteristic features of electron transport through extended states, albeit with relatively low mobility ($\mu \sim 0.1$ m^2 V^{-1} s^{-1} at $T = 293$ K) due to scattering of electrons by N atoms. In contrast, at large electric fields (>1 kV cm^{-1}), the conduction electrons gain sufficient energy to approach the energy of the resonant N level, where they become spatially localized. This resonant electron localization in an electric field (RELIEF) leads to negative differential velocity. The RELIEF effect could be observed in other III–N–V compounds, such as $InAs_{1-x}N_x$ and $InP_{1-x}N_x$, and has potential for applications in terahertz electronics.

1. Introduction

Progress in the synthesis and engineering of semiconductor materials has led to improved device performances and functionalities. In particular, in the last decade, there has been considerable interest in the physics and applications of highly-mismatched alloys in which small and highly-electronegative isovalent N atoms are incorporated onto the anion sublattice of a III–V compound semiconductor [1]. The most studied material is the $GaAs_{1-x}N_x$ alloy, where a small percentage of N ($x < 1\%$) perturbs dramatically the electronic properties of the host GaAs crystal leading to a large reduction of the fundamental energy band gap [2], an increase of the electron effective mass [3, 4] and an unusual response of these properties to hydrostatic pressure [5, 6]. These effects differ from the smoother variation of the energy band gap and electron effective mass with alloy composition observed in other semiconductor compounds, such as $In_yGa_{1-y}As$. The incorporation of N in GaAs gives rise to a qualitatively different type of alloy phenomenon: N impurities and N clusters tend to localize the extended Bloch states of GaAs at resonant energies in the conduction band (CB) [7], thus fragmenting the energy–wavevector dispersion relations [8–10].

The possibility of tailoring the electronic properties of III–V compounds by N incorporation has stimulated proposals for innovative devices in optoelectronics [11], band gap nano-engineering [12] and high-frequency (terahertz, THz) electronics [13]. However, to date, the implementation of dilute nitrides in these technologies presents several challenges, including a degradation of the electron mobility, μ [14, 15]. Also, despite a rapidly expanding body of work on the electronic properties of $GaAs_{1-x}N_x$ [2], the range of N concentrations over which this alloy behaves as a good conductor is not yet well established.

In this paper, we investigate how the incorporation of N in GaAs affects the electrical conductivity. Our studies in n-type $GaAs_{1-x}N_x$ epilayers reveal a large increase of the resistivity, ρ, for $x > 0.2\%$, which we attribute to the emergence of defect states with deep ($\sim$0.3 eV) energy levels. Electron

trapping onto these states is not observed at low x ($x \leqslant 0.2\%$). In this ultra-dilute alloy regime and at low electric fields ($F < 1$ kV cm^{-1}) the electrical conductivity retains the characteristic features of transport through extended states, albeit with relatively low mobility ($\mu \sim 0.1$ m^2 V^{-1} s^{-1} at $T = 293$ K) due to scattering of electrons by N atoms. We focus on this ultra-dilute regime and exploit the admixing of the localized single N impurity level with the extended conduction band states of GaAs to realize an unusual type of negative differential velocity (NDV) effect: at large F (>1 kV cm^{-1}), electrons gain sufficient energy to approach the energy of the resonant N level, where they become spatially localized. This resonant electron localization in electric field, to which we give the acronym RELIEF, leads to NDV and strongly non-linear current–voltage characteristics $I(V)$. We envisage that the RELIEF effect could be observed in other III–N–V alloys, such as $InP_{1-x}N_x$ and $InAs_{1-x}N_x$. In these compounds the nature of the resonant interaction between the N level and the conduction band states of the host crystal is still relatively unexplored [16, 17]. However, it is clear that the different energy positions of the N level relative to the conduction band minimum of different materials could offer new degrees of freedom in the design of the electronic band structure and electron dynamics.

The RELIEF effect may open up prospects for future applications in fast electronics. We discuss the maximum response frequency, f_{max}, of a RELIEF diode and show that this can be tuned by the applied electric field in the THz frequency range. This is of potential technological significance for the development of detectors/sources in the 0.6–1 THz region, which is not easily attainable using conventional transferred electron devices (TEDs) [18] and quantum cascade lasers [19].

2. Samples

For these studies, we used a series of planar n-doped $GaAs_{1-x}N_x$ epilayers grown by molecular beam epitaxy on semi-insulating (100)-oriented GaAs substrates with $x = 0$, 0.1, 0.2, 0.4 and 1%. The growth sequence is as follows: a 20 nm-thick undoped GaAs buffer layer (growth temperature $T_G = 580\,^\circ$C) and an n-type $GaAs_{1-x}N_x$ layer of thickness $t = 1\ \mu$m, doped with Si to 1×10^{23} m^{-3} ($T_G = 500\,^\circ$C). We have also investigated a number of structures based on $GaAs_{1-x}N_x$ epilayers with different n-type doping (Si: 1×10^{24} m^{-3} and Se: 1×10^{25} m^{-3}) [20], modulation doped $GaAs_{1-x}N_x$ quantum wells [20, 21] and n$^+$–n–n$^+$ GaAs/$GaAs_{1-x}N_x$/GaAs diodes in which the current flows perpendicular to the growth plane [22]. Our previous studies [20–22] focused on structures with small N concentrations ($x \sim 0.1\%$). Here we consider n-doped $GaAs_{1-x}N_x$ epilayers with a wider range of x and investigate how the incorporation of N in GaAs changes the electrical conductivity in both the low and high F-regime.

For measurements at low F (<1 kV cm^{-1}), all samples were processed into Hall bars. For high-F and NDV studies, we fabricated two terminal planar devices with small areas to minimize heating effects. These diodes incorporate a conducting channel of length $L = 1$, 2, 5 or 10 μm and of width $W = 1$, 2 or 5 μm. Devices with different geometries share the same electrical properties (i.e. same resistivity, mobility and critical electric field for NDV). Here we focus on high-field data for a device with $L = 10\ \mu$m and $W = 1\ \mu$m. We have performed photoluminescence (PL) experiments on all samples to assess the N-induced modification of the optical properties. For PL experiments, the optical excitation was provided by the 514.5 nm line of an Ar$^+$ laser. The luminescence was dispersed by a 1/2 m monochromator and detected by a cooled (InGa)As photodiode.

3. Experiments and analysis

3.1. Resistivity measurements

Figure 1(a) shows values of resistivity, ρ, at different T and $B = 0$ for a series of $GaAs_{1-x}N_x$ epilayers with different x. These data reveal a strong increase of ρ at $x > 0.2\%$, which becomes steeper with decreasing T. Samples with $x > 0.2\%$ have resistivities well above the minimum value, ρ_{min}, for the disorder-induced metal–insulator transition. This is given by $\rho_{min} = (3\pi^2)^{2/3}\hbar e^{-2} n_e^{-1/3} \sim h\lambda_F/e^2$, where n_e is the free electron density and λ_F is the Fermi wavelength [23]. The low resistivity for $x > 0.2\%$ is accompanied by a thermally activated behavior of ρ, see figure 1(b). Also an increase of x above 0.2% leads to a pronounced quenching and red shift of the PL emission, see figure 1(c).

As shown in figure 1(b), for $x > 0.2\%$ the resistivity follows an exponential dependence of the type $\rho(T) \sim \exp(\Delta E/k_B T)$, where $\Delta E = (0.15 \pm 0.01)$ eV is a characteristic activation energy into the conduction band. This T-dependence indicates that for $x > 0.2\%$, the electronic transport is largely governed by trapping of electrons onto localized states below the CB edge. Correspondingly, we find that the free electron concentration derived from Hall measurements ($n_e \sim 4 \times 10^{21}$ m^{-3} at $T = 293$ K) is considerably smaller than the nominal value (1×10^{23} m^{-3}) expected from the level of Si-doping, thus suggesting trap densities as high as 10^{23} m^{-3}. This high concentration of traps indicates that the chemical potential is somewhere between the energy level of the localized states and the CB edge. Thus, for $x > 0.2\%$, the binding energy E_b of the electron trap is approximately equal or larger than ΔE. This is consistent with the value of $E_b \sim 0.25$ eV extracted from recent PL studies of nominally undoped $GaAs_{1-x}N_x$ epilayers [24] and attributed to a complex involving a Ga-vacancy (V_{Ga}) and a N antisite (N_{Ga}) [25, 26]. The concentration of these acceptor complexes increases with N content [24–26], in agreement with the strong reduction of the free electron density and PL intensity observed in our samples at $x > 0.2\%$ (figure 1(c)).

The marked increase of ρ at $x > 0.2\%$ is a clear manifestation of the degradation of the crystal quality and electrical properties due to the emergence of crystal defects arising from the N incorporation. We find that the transition from metallic to insulating behavior at $x > 0.2\%$ becomes less pronounced for higher n-type (Si or Se $\geqslant 1 \times 10^{24}$ m^{-3}) doping [20] due to a smaller compensation effect. However,

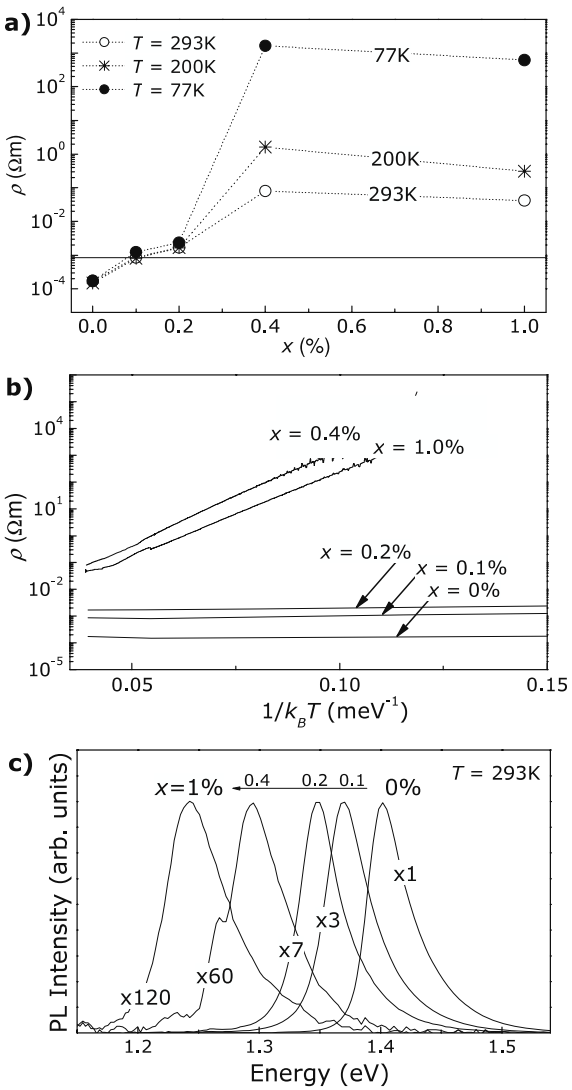

Figure 1. (a) Resistivity, ρ, versus x at different T ($B = 0$). The horizontal line shows the minimum resistivity, $\rho_{\min}$, for the disorder-induced metal–insulator transition. Dotted lines are guides to the eye. (b) Dependence of ρ versus $1/k_BT$ at different x. (c) Normalized PL spectra at $T = 293$ K.

we also note that the increase of ρ at $x > 0.2\%$ does not correlate with the measured decrease of the Hall mobility, μ. As shown in figure 2, the N-induced quenching of the Hall mobility manifests itself in the ultra-dilute regime ($x \sim 0.1\%$) and tends to saturate at $x > 0.2\%$. Note that μ is 0.03 m^2 V^{-1} s^{-1}, independent of x for $x > 0.2\%$. This dependence was also observed in several samples based on modulation doped $GaAs_{1-x}N_x$-quantum wells and Si-doped $GaAs_{1-x}N_x$ epilayers reported by other groups and ourselves [20, 27–29], see figure 2.

To understand the mobility data, we first consider a simple model developed by Fahy and O'Reilly [30] in which μ is controlled by scattering of electrons by a random distribution of N atoms and is expressed as

$$\mu^{-1} = \frac{\sqrt{3m_e^* k_B T}}{e}\pi\left(\frac{m_e^*}{2\pi\hbar^2}\right)^2\left(\frac{dE_c}{dx}\right)^2 a^3 x, \qquad (1)$$

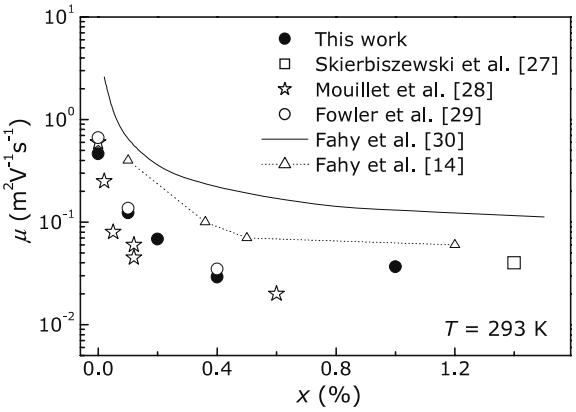

Figure 2. Dependence of μ on x at $T = 293$ K: comparison of experimental data with theory. Symbols refer to samples from this work (full dots) and from the literature. The continuous line is the calculated mobility from [30]. The dotted line is a guide to the eye.

where k_B is the Boltzmann constant, e is the electron charge, a is the GaAs lattice constant, E_c is the CB edge energy of $GaAs_{1-x}N_x$ and m_e^* is the electron effective mass. Here E_c and m_e^* are calculated using a two-level band anticrossing (BAC) model [1]. Using equation (1) and the BAC model, we find that the x-dependence of μ is mainly governed by the rate of change of E_c with x. As shown in figure 2, this dependence describes the characteristic saturation behavior of the measured mobility at large x, although it fails to reproduce it quantitatively. A better agreement between theory and experiment is obtained by taking into account the unusual type of alloy disorder induced by the N incorporation in GaAs: N atoms tend to form N–N pairs and N clusters with resonant energy levels in the conduction band; elastic scattering of the conduction electrons by these resonant states causes a strong reduction of μ [14]. As shown in figure 2, for $x \sim 1\%$, this resonant scattering model predicts $\mu = 0.06$ m^2 V^{-1} s^{-1} at $T = 293$ K in quite good agreement with the measured value ($\mu = 0.04$ m^2 V^{-1} s^{-1} for $T = 293$ K).

In the next section, we focus on the ultra-dilute regime of N concentrations ($x \sim 0.1\%$) for which N clusters and/or other crystal defects play a minor role. In this regime, we exploit the unique electronic band structure of $GaAs_{1-x}N_x$ to induce a resonant electron localization in electric field (RELIEF).

3.2. RELIEF effect

The RELIEF effect is based on the idea of accelerating electrons to larger energies in the CB by a means of a strong electric field. Here they become resonantly localized onto the N levels, leading to a negative differential velocity effect. To describe the RELIEF effect, we use a semiclassical model for the electron motion and a BAC model for the energy dispersion $\varepsilon(k)$ curves of the conduction band of $GaAs_{1-x}N_x$, see figure 3(a). In the BAC model, the admixing and hybridization of the extended conduction band states of GaAs with the localized single N impurity levels causes a splitting of the conduction band into two subbands, E_- and E_+, with strongly non-linear energy dispersions [1]. Our previous

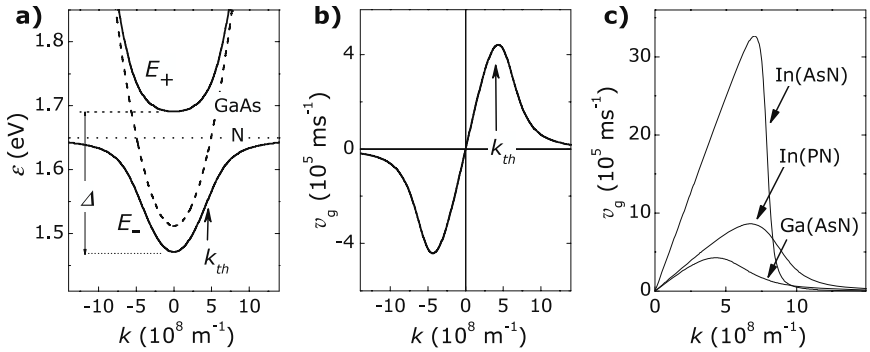

Figure 3. $\varepsilon(k)$ curve for subbands E_- and E_+ of $GaAs_{1-x}N_x$ ($x = 0.1\%$). (b) $v_g(k)$ curve for electrons in the E_- subband of $GaAs_{1-x}N_x$ ($x = 0.1\%$). (b) $v_g(k)$ curves for various III–N–V alloys with $x = 0.1\%$. All curves are calculated using the BAC model with parameters from [16].

magneto-tunneling spectroscopy experiments [8, 10] provided a means of probing this band structure at low x ($\sim$0.1%) and demonstrated that the BAC model offers a simple approach and a valid physical picture of the electronic properties, even though it does not describe the details of the localized character of the N-induced states [7, 9]. In the following section we discuss the validity and limitations of the BAC model in the description of the electronic transport of $GaAs_{1-x}N_x$ in the high-field regime.

Figure 3(b) shows the group velocity, $v_g(k) = \hbar^{-1}(\partial\varepsilon/\partial k)$, for electrons in the lower energy hybridized subband, E_-. The group velocity has a maximum at the inflection point of the $\varepsilon(k)$ curve at a given critical k-value, k_{th}, and falls off rapidly at higher k. The unusual form of the $v_g(k)$ curve arises from the resonant interaction between the conduction band states of GaAs and the randomly-positioned N atoms, which leads to resonant localization of electrons at relatively modest wavevectors, considerably smaller ($\sim$10%) than the size of the Brillouin zone of the crystal lattice. The nature of this resonance in other III–V materials, such as $InP_{1-x}N_x$ and $InAs_{1-x}N_x$, is still unexplored territory. In these alloys, the anticrossing effect is expected to occur at higher electron energies. Therefore, in these compounds it should be possible to achieve peak velocities considerably larger than those in $GaAs_{1-x}N_x$, but with similar and easily achievable values of k_{th}, see figure 3(c).

The electronic band structure of dilute nitrides has interesting implications for the dynamics of conduction electrons when an applied dc electric field, F, accelerates them towards increasing k-vectors. We derive the dependence on time, t, of the average energy, $\bar{\varepsilon}(t)$, and of the drift velocity, $v_d(t)$, by solving the dynamical balance equations [31–33]:

$$\frac{dv_d}{dt} = \frac{qF}{m_e^*(\bar{\varepsilon})} - r_v v_d, \tag{2}$$

$$\frac{d\bar{\varepsilon}}{dt} = qFv_d - r_i\bar{\varepsilon}. \tag{3}$$

Here q ($= -e$) is the electron charge, $r_v = r_i + r_e$ is the relaxation rate of the velocity, which includes the energy relaxation rate, r_i, and the elastic scattering rate, r_e, and $m_e^*(\bar{\varepsilon})$ is the energy-dependent electron effective mass derived from the functional form of the $E_-(k)$ dispersion. The steady state solution of equations (2) and (3) leads to the following relations $v_d = r_i\bar{\varepsilon}/qF$ and $\bar{\varepsilon} = q^2F^2/(m_e^*(\bar{\varepsilon})r_v r_i)$, from which we derive numerically the drift velocity-field characteristic, $v_d(F)$. According to this model, for any value of F, the average electron energy $\bar{\varepsilon}$ is always smaller than the energy ε_{th} of the electron at the inflection point k_{th} of the $E_-(k)$ curve. For $\bar{\varepsilon} < \varepsilon_{th}$, the electron effective mass can be approximated by $m_e^*(\bar{\varepsilon}) = m_e^*(0)/(1 - \bar{\varepsilon}/\varepsilon_{th})$. Using this expression, we find that $v_d(F)$ reduces to the form

$$v_d(F) = \mu F/[1 + (F/F_T)^2], \tag{4}$$

where $\mu = e/(m_e^*(0)r_v)$ is the low-field mobility, $F_T = p_N(r_v r_i)^{1/2}(1 + D)^{1/4}/2e$ is the critical field corresponding to a peak drift velocity $v_d^M = p_N(r_i/r_v)^{1/2}(1 + \sqrt{1 + D})/8m_0(1 + D)^{1/4}$, $p_N = \sqrt{2m_0\Delta_N}$, Δ_N is the energy position of the N level relative to the CB minimum of GaAs ($\Delta_N = 0.13$ eV), m_0 is the electron effective mass of GaAs at $k = 0$, $D = 4V_{NM}^2/\Delta_N^2$ and $V_{NM} = C_{NM}x^{1/2}$ ($C_{NM} = 2.7$ eV) is the coupling matrix element between the N level and the CB states of GaAs in the BAC model.

This semiclassical model provides a good description of the RELIEF and negative differential conductance (NDC) effects previously observed in modulation doped $GaAs_{1-x}N_x$ quantum wells [21] and in n^+–n–n^+ GaAs/$GaAs_{1-x}N_x$/GaAs heterostructures [22] with $x = 0.1\%$. The similarity of the NDC effect in all these structures indicates that it arises from a common mechanism, namely RELIEF, rather than from real space charge transfer [34]. To explore the RELIEF effect in n-type $GaAs_{1-x}N_x$ epilayers over a wider range of x, we prepared a series of small planar devices with short and narrow channels, as shown in the inset of figure 4 for a structure with channel length $L = 10$ μm and width $W = 1$ μm. As shown in figure 4, the low temperature ($T = 77$ K) $I(V)$ of diodes with $x = 0$, 0.1 and 0.2% exhibit an ohmic behavior at low bias, followed by a sublinear V-dependence of the current or a region of NDC for biases above a threshold value V_T. Samples with $x = 0.4$ and 1% show a similar saturation of the $I(V)$, but at much larger applied biases.

The NDC observed for the GaAs diode ($x = 0\%$) is due to the well-known transfer electron (Gunn) effect [18].

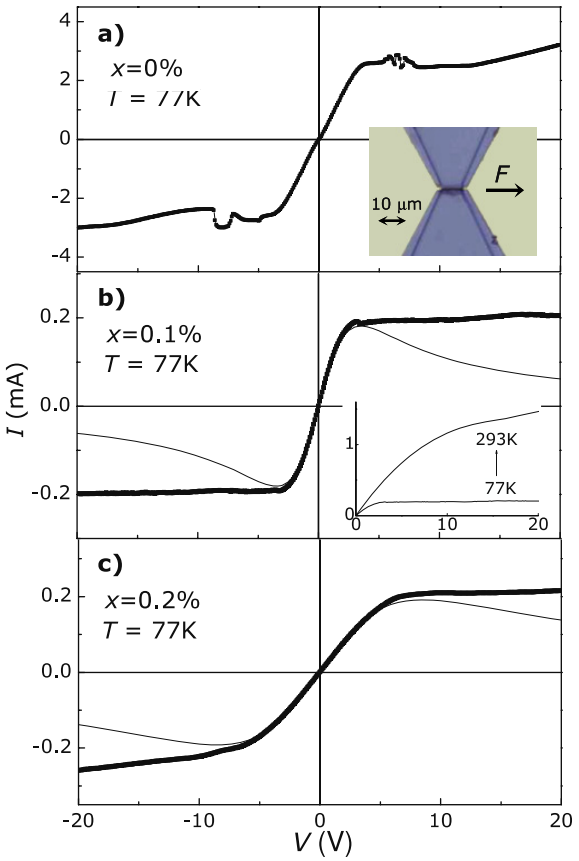

Figure 4. (a)–(c) Measured $I(V)$ at $T = 77$ K for $GaAs_{1-x}N_x$ with $x = 0$, 0.1 and 0.2%. Continuous lines in parts (b) and (c) are the $I(V)$ curves calculated using the semiclassical model and parameters described in the text. Inset in part (a) shows an optical microscope image of one device. Inset in part (b) compares the measured $I(V)$ curves at $T = 77$ K and 293 K for $x = 0.1\%$.

(This figure is in colour only in the electronic version)

The critical field for NDC is $F_T = V_T/L = 5$ kV cm^{-1} at $T = 77$ K and is consistent with the typical values expected for Gunn diodes based on n-doped GaAs. For $GaAs_{1-x}N_x$ samples, the measured $I(V)$ curves can be instead described in terms of the $v_d(F)$ characteristics predicted by our model. In figure 4 we plot the $I(V)$ curves calculated from $v_d(F)$ using the relations $V = FL$ and $I = n_e e v_d W t$, where $t = 1$ μm is the thickness of the $GaAs_{1-x}N_x$ epilayer, $W = 1$ μm is channel width and n_e is the electron density derived from Hall measurements. Each theoretical curve is obtained by using the low-field mobility, μ, and the critical field, F_T, as fitting parameters. Our fit to the data gives $\mu = 0.16$ m^2 V^{-1} s^{-1} and $F_T = 3.5$ kV cm^{-1} for $x = 0.1\%$, and $\mu = 0.07$ m^2 V^{-1} s^{-1} and $F_T = 8.5$ kV cm^{-1} for $x = 0.2\%$. These values of μ are close to those obtained from Hall measurements on standard Hall bars ($\mu = 0.13$ and 0.08 m^2 V^{-1} s^{-1} for $x = 0.1\%$ and 0.2%, respectively) and correspond to a scattering rate $r_v = e/m_e^*(0)\mu = 1.5 \times 10^{13}$ and 3.1×10^{13} s^{-1} for $x = 0.1\%$ and 0.2%, respectively. The large values of r_v are consistent with strong elastic scattering due to collisions of electrons by the N atoms. The increasing elastic scattering with increasing x tends to shift F_T to higher values. In modeling the $I(V)$ curves, we have neglected space charge effects. These become increasingly important with increasing bias and can account for the saturation behavior of the $I(V)$ curve at high V.

We note that for $x > 0$, increasing T above 77 K leads to a large increase of F_T and of the high-bias current, see inset of figure 4(b). This T-dependence differs from that observed in our GaAs control sample ($x = 0\%$) where thermal effects are much weaker and consistent with those expected for Gunn diodes [35]. To understand these data, we first consider the effect of the electron energy distribution on the velocity–electric field curves. The analysis of the energy distribution function derived from the Boltzmann equation indicates that increasing electric field gives rise to a broadening of the distribution function in momentum space. However, this approach leads to almost identical velocity–electric field curves to those derived when broadening is neglected. We also note that, due to the large energy gap Δ_G between the E_- and E_+ subbands ($\Delta_G \geqslant 50$ meV for $x \geqslant 0.1\%$), Zener tunneling of electrons between the two subbands becomes important only at electric fields much larger than those required to reveal the NDR effect.

Although our model for the drift velocity calculation gives us a clear physical picture of the RELIEF effect, it neglects the hybridized nature of the electronic states and their increasingly localized character as their energy approaches that of the resonant N level. These states have finite probability to either capture or release conduction electrons, both processes being influenced by temperature. The N-induced localized states and the thermal excitation of electrons out of these states could explain the stronger T-dependence of the $I(V)$ curves at $x > 0$. This effect merits further investigation and theoretical modeling.

Finally, we note that the RELIEF effect should also be present in other III–N–V alloys and/or quantum confined systems. By designing quantum confined structures incorporating a range of different alloys, N concentration, strength of electron confinement and n-type doping, it may be possible to fine-tune the form of the dispersion curves and achieve accurate control of the $v_d(F)$ and $I(V)$ curves. In previous studies [5] we have demonstrated that hydrostatic pressure provides a test-bed of this band engineering concept. The pressure-induced increase of the CB edge energy of GaAs relative to the localized N level leads to a marked flattening of the $\varepsilon(k)$ dispersion curve and hence to a different k-dependence of the electron group velocity [5]. This observation suggests that engineering of the energy dispersions using different alloys and/or quantum confined systems offers a realistic opportunity for controlling the RELIEF effect and the corresponding ac electron dynamics, which we discuss in the following section.

3.3. RELIEF and high-frequency electronics

The ac dynamics associated with the RELIEF effect is fundamentally different from that occurring in conventional systems, such as semiconductor superlattices [36] and transfer electron (Gunn) diodes [18] based on III–V compounds. In striking contrast to the case of superlattices, the transient

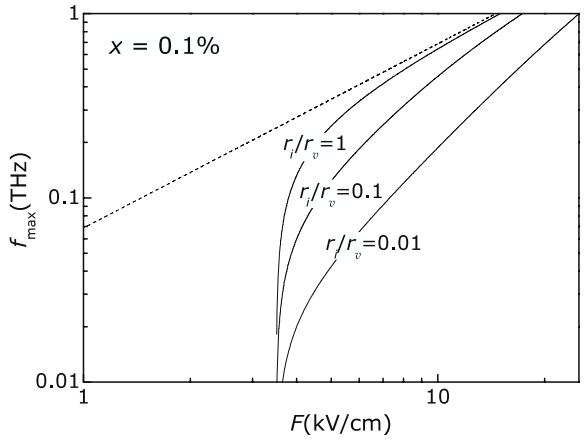

Figure 5. Dependence of $f_{\max}$ on dc electric field F for $GaAs_{1-x}N_x$ ($x = 0.1\%$), $F_T = 3.5$ kV cm^{-1} and $\delta r_i/r_v = 0.01$, 0.1 and 1 (continuous lines). The dashed line describes the F-dependence of $\tilde{f} = 1/2\pi\tilde{\tau}$, where $\tilde{\tau}$ is the time of ballistic acceleration of electrons to the inflection point k_{th} in the $\varepsilon(k)$ curve of the E_- subband.

ballistic response of the electron velocity in $GaAs_{1-x}N_x$ does not reveal time-domain Bloch oscillations. The electron dynamics also differs from that occurring in GaAs-based TEDs in which the dynamics is controlled by electron transfer from the Γ-to the L-valleys of the conduction band. The aim of this section is to understand how the ac dynamics in $GaAs_{1-x}N_x$ is governed by the electronic band structure and by the balance between the driving force of the electric field and the relaxation of electron energy and momentum due to resonant localization and inelastic/elastic scattering processes.

We model the ac response of electrons in $GaAs_{1-x}N_x$ by solving the dynamical balance equations (2) and (3) with a field $\tilde{F}$, which comprises a dc field F and a small alternating sinusoidal field with amplitude $F_1 \ll F$ and angular frequency ω, i.e. $\tilde{F}(t) = F + F_1 \exp(i\omega t) + \text{c.c.}$ This allow us to derive an expression for the electron drift velocity $\tilde{v}_d(t) = v_d + v_1 \exp(i\omega t) + \text{c.c.}$, where $v_1(t) = \mu(\omega, F)F_1$ and $\mu(\omega, F)$ is a complex differential mobility [13]. The onset of generation/amplification of high-frequency radiation in the absence of external losses and perfect matching of the generating system to an external circuit is given by the condition that the work, W, done by the ac field on electrons is negative. For small sinusoidal electric fields, this condition can be written as $W = 2\mu_r(f, F)|F_1|^2 < 0$ or $\mu_r(f, F) < 0$, where $\mu_r(\omega, F)$ is the real part of $\mu(\omega, F)$ and $f = \omega/2\pi$. Using this condition, we find that the maximum frequency, $f_{\max}$, associated with the NDV in $GaAs_{1-x}N_x$ can be expressed as

$$f_{\max} = \frac{1}{2\pi\tilde{\tau}(F)(F/F_T)}\left[\frac{(F/F_T)^4 - 1}{(F/F_T)^2 + \delta^{-1}}\right]^{1/2}, \qquad (5)$$

where $\delta = r_i/r_v$ and $\tilde{\tau}(F) = \sqrt{m_e^*(0)\varepsilon_{th}}/eF \sim \hbar k_{th}/eF$ is the field-dependent characteristic time of ballistic acceleration of electrons to the inflection point at k_{th} in $E_-(k)$. Figure 5 shows the dependence of $f_{\max}$ on F for $x = 0.1\%$, $F_T = 3.5$ kV cm^{-1} and increasing values of $\delta = r_i/r_v$. For a given δ, $f_{\max}$ increases rapidly for $F > F_T$ and, in the limit $F \gg F_T$, it approaches a maximum value $\tilde{f} = 1/2\pi\tilde{\tau}$. For a given F, $f_{\max}$ decreases with decreasing δ. From figure 5 it can be also seen that for a critical field F_T equal to that measured in our sample at $x = 0.1\%$, the applied electric field provides a means of tuning $f_{\max}$ up to THz frequencies.

Our semiclassical model of the electron motion gives us a simple physical picture for the ac dynamics in $GaAs_{1-x}N_x$. This arises from the unique CB structure of this alloy in which a full energy gap exists for electron motion in *all* spatial directions. Since electrons can be accelerated very quickly ($\tilde{\tau} < 1$ ps at $F > F_T$) by an electric field towards this energy gap, the ac response of electrons can be fast (∼THz) and is limited only by scattering. Our recent studies of $GaAs_{1-x}N_x$ have already shown a fast response of the current in the sub-THz frequency range [37]. Experiments involving diodes optimized for THz-operation coupled with a quantitative theoretical model of the THz dynamics will be now needed to assess the use of $GaAs_{1-x}N_x$ and other III–N–V alloys in detectors/sources of THz radiation.

4. Conclusion

In conclusion, we have shown that the addition of nitrogen to the lattice of n-type GaAs acts to modify the electrical conductivity at both low and high electric fields. The electronic conduction is suppressed at $x > 0.2\%$ due to freezing of the conduction electrons onto deep crystal defects. These tend to compensate the n-type dopants by trapping electrons, thus leading to insulating behavior. These defects play a minor role at small x ($\leqslant 0.2\%$). In this ultra-dilute regime, we have demonstrated that the resonant interaction between the N level and the extended conduction band states of GaAs leads to an unusual resonant localization of electrons in electric field (RELIEF). The investigation of the RELIEF effect in other III–N–V alloys and the possibility of finely manipulating the electron dynamics by N atoms could greatly broaden and enhance our knowledge of this class of materials and could contribute to the development of new technologies based on high-frequency electronics. We predict that the maximum response frequency associated with the RELIEF effect in $GaAs_{1-x}N_x$ can be tuned by the applied electric field in the THz frequency range. This region of the electromagnetic spectrum is often referred to as the THz gap due to the unfulfilled need for compact, solid state devices that can emit radiation in this frequency range in a selectable and tuneable way. Therefore $GaAs_{1-x}N_x$ and other III–N–V alloys could open up new opportunities in this topical research area of device physics.

Acknowledgments

We thank the Engineering and Physical Sciences Research Council (UK), the Royal Society (UK), the Russian Foundation for Basic Research and the Russian Academy of Sciences for their support.

References

[1] Shan W, Walukiewicz W, Ager J W, Haller E E, Geisz J F, Friedman D J, Olson J M and Kurtz S R 1999 Band anticrossing in GaInNAs alloys *Phys. Rev. Lett.* **82** 1221

[2] Henini M 2004 *Dilute Nitride Semiconductors* (London: Elsevier)

[3] Masia F, Pettinari G, Polimeni A, Miriametro A, Capizzi M, Lindsay A, Healy S B, O'Reilly E P, Cristofoli A, Bais G, Piccin M, Rubini S, Martelli F, Franciosi A, Klar P J, Volz K and Stolz W 2006 Interaction between conduction band edge and nitrogen states probed by carrier effective-mass measurements in $GaAs_{1-x}N_x$ *Phys. Rev.* B **73** 073201

[4] Allison G, Spasov S, Patanè A, Eaves L, Koslova N, Freudemberger J, Hopkinson M and Hill G 2008 Electron effective mass and Si-donor binding energy in $GaAs_{1-x}N_x$ probed by a high magnetic field *Phys. Rev.* B **77** 125210

[5] Endicott J, Patanè A, Maude D, Eaves L, Hopkinson M and Hill G 2005 Effect of hydrostatic pressure on the fragmented conduction band structure of dilute Ga(AsN) alloys *Phys. Rev.* B **72** 041306(R)

[6] Pettinari G, Polimeni A, Masia F, Trotta R, Felici M, Capizzi M, Niebling T, Stolz W and Klar P J 2007 Electron mass in dilute nitrides and its anomalous dependence on hydrostatic pressure *Phys. Rev. Lett.* **98** 146402

[7] Kent P R C and Zunger A 2001 Theory of electronic structure evolution in GaAsN and GaPN alloys *Phys. Rev.* B **64** 115208

[8] Endicott J, Patanè A, Ibanez J, Eaves L, Bissiri M, Hopkinson M, Airey R and Hill G 2003 Magnetotunneling spectroscopy of dilute Ga(AsN) quantum wells *Phys. Rev. Lett.* **91** 126802

[9] Lindsay A and O'Reilly E P 2004 Unification of the band anticrossing and cluster-state models of dilute nitride semiconductor alloys *Phys. Rev. Lett.* **93** 196402

[10] Patanè A, Endicott J, Ibáñez J, Eaves L, Brunkov P N, Healy S B, Lindsay A, O'Reilly E P and Hopkinson M 2005 Breakup of the conduction band structure of dilute $GaAs_{1-y}N_y$ alloys *Phys. Rev.* B **71** 195307

[11] Adams A R 2004 Band-structure engineering to control impact ionisation and related high-field processes *Electron. Lett.* **40** 1086

[12] Felici M, Polimeni A, Salviati G, Lazzarini L, Armani N, Masia F, Capizzi M, Martelli F, Lazzarino M, Bais G, Piccin M, Rubini S and Franciosi A 2006 In-plane bandgap engineering by modulated hydrogenation of dilute nitride semiconductors *Adv. Mater.* **18** 1993

[13] Ignatov A, Patanè A, Makarovsky O and Eaves L 2006 Terahertz response of hot electrons in dilute nitride Ga(AsN) alloys *Appl. Phys. Lett.* **88** 032107

[14] Fahy S, Lindsay A, Ouerdane H and O'Reilly E P 2006 Alloy scattering of n-type carriers in GaN_xAs_{1-x} *Phys. Rev.* B **74** 035203

[15] Vaughan M P and Ridley B K 2007 Electron–nitrogen scattering in dilute nitrides *Phys. Rev.* B **75** 195205

[16] Vurgaftman I and Meyer J R 2003 Band parameters for nitrogen-containing semiconductors *J. Appl. Phys.* **94** 3675

[17] Veal T D, Piper L F J, Jefferson P H, Mahboob I, McConville C F, Merrick M, Hosea T J C, Murdin B N and Hopkinson M 2005 Photoluminescence spectroscopy of bandgap reduction in dilute InNAs alloys *Appl. Phys. Lett.* **87** 182114

[18] Ridley B K and Watkins T B 1961 Possibility of negative resistance effects in semiconductors *Proc. Phys. Soc.* **78** 293
Hilsum C 1962 Transferred electron amplifiers and oscillators *Proc. Inst. Radio Engineers* **50** 185
Gunn J B 1963 Microwave oscillations of current in III–V semiconductors *Solid State Commun.* **1** 88

[19] Walther C, Fischer M, Scalari G, Terazzi R, Hoyler N and Faist J 2007 Quantum cascade lasers operating from 1.2 to 1.6 THz *Appl. Phys. Lett.* **91** 131122

[20] Fowler D, Makarovsky O, Patanè A, Eaves L, Geelhaar L, Reichert H and Uesugi K 2005 *ICPS-27: The 27th Int. Conf. on the Physics of Semiconductors*; *AIP Conf. Proc.* **772** 497

[21] Patanè A, Ignatov A, Fowler D, Makarovsky O, Eaves L, Geelhar L and Riechert H 2005 Hot-electrons and negative differential conductance in $GaAs_{1-x}N_x$ *Phys. Rev.* B **72** 033312

[22] Allison G, Spasov S, Patanè A, Eaves L, Ignatov A, Maude D, Hopkinson M and Airey R 2007 Magnetophonon oscillations in the negative differential conductance of dilute nitride $GaAs_{1-x}N_x$ submicron diodes *Phys. Rev.* B **75** 115325

[23] Lee P A and Ramakrishnan T V 1985 Disordered electronic systems *Rev. Mod. Phys.* **57** 287

[24] Bentoumi G, Yaiche Z, Leonelli R, Beaudry J-N, Desjardins P and Masut R A 2008 Low-temperature emission in dilute GaAsN alloys grown by metalorganic vapor phase epitaxy *J. Appl. Phys.* **103** 063526

[25] Janotti A, Wei S-H, Zhang S B, Kurtz S and Van de Walle C G 2003 Interactions between nitrogen, hydrogen, and gallium vacancies in $GaAs_{1-x}N_x$ alloys *Phys. Rev.* B **67** 161201

[26] Toivonen J, Hakkarainen T, Sopanen M, Lipsanen H, Oila J and Saarinen K 2003 Observation of defect complexes containing Ga vacancies in GaAsN *Appl. Phys. Lett.* **82** 40

[27] Skierbiszewski C, Perlin P, Wisniewski P, Suski T, Walukiewicz W, Shan W, Ager J W, Haller E E, Geisz J F, Friedman D J, Olson J M and Kurtz S R 1999 Effect of nitrogen-induced modification of the conduction band structure on electron transport in GaAsN alloys *Phys. Status Solidi* b **216** 135

[28] Mouillet R, de Vaulchier L A, Deleporte E, Guldner Y, Travers L and Harmand J-C 2003 Role of nitrogen in the mobility drop of electrons in modulation-doped GaAsN/AlGaAs heterostructures *Solid State Commun.* **126** 333

[29] Fowler D, Makarowsky O, Patanè A, Eaves L, Geelhaar L and Reichert H 2004 Electron conduction in two-dimensional $GaAs_{1-y}N_y$ channels *Phys. Rev.* B **69** 153305

[30] Fay S and O'Reilly E P 2003 Intrinsic limits on electron mobility in dilute nitride semiconductors *Appl. Phys. Lett.* **83** 3731

[31] Ignatov A A and Romanov Yu A 1976 Nonlinear electromagnetic properties of semiconductors with a superlattice *Phys. Status Solidi* b **73** 327

[32] Büttiker M and Thomas H 1977 Current instability and domain propagation due to Bragg scattering *Phys. Rev. Lett.* **38** 78

[33] Ignatov A A, Renk K F and Dodin E P 1993 Esaki–Tsu superlattice oscillator-Josephson-like dynamics of carriers *Phys. Rev. Lett.* **70** 1996

[34] Ridley B K 1991 Hot electrons in low dimensional structures *Rep. Prog. Phys.* **54** 169

[35] Higashisaka A 1970 Temperature dependence of Gunn effect in GaAs over range 77–545 K *Japan. J. Appl. Phys.* **9** 583

[36] Tsu R 2005 *Superlattice to Nanoelectronics* (Amsterdam: Elsevier)

[37] Spasov S, Allison G, Patanè A, Eaves L, Tretyakov M, Ignatov A, Hopkinson M, Hill G and Airey R 2008 High field electron dynamics in dilute nitride GaAsN *Appl. Phys. Lett.* **93** 022111